Advances in Chemical Engineering

Chapter 2

Hydroxyapatite Applications in Environmental Monitoring and Treatment

Yanni Tan[1*]; Yanjun Liu[1]; Songzhu Luo[1]; Junqi Li[2]

[1]State Key Laboratory of Powder Metallurgy, Central South University, Changsha 410083, China

[2]Yuanmeng Precision Technology (Shenzhen) Institute, Shenzhen 518055, China

***[*]Correspondence to: Yanni Tan,** State Key Laboratory of Powder Metallurgy, Central South University, Changsha 410083, China*

Email: tanyanni@csu.edu.cn

1. Introduction

Hydroxyapatite (HAp, $Ca_{10}(PO_4)_6(OH)_2$) is well-known for its important role in the body of the vertebrate, including human beings. HAp amounts 70% of bones and human teeth also mainly consist of nano HAp rods [1,2]. HAp makes them more stable and harder so that they can function. Thus, it is not surprising that HAp is a widely-used biomaterial with great biocompatibility. Besides the biological applications [3,4], HAp can also serve as a long-term assurance material for radioactive waste [5], fluorescent lamps [6], gas sensors [7], adsorbents for heavy metals [8] and catalysis [9]. All of its diverse applications are contributed to its variability of properties, which is closely linked to its unique structure. In this chapter, we are focusing on the applications of HAp in the field of environmental monitoring and treatment, including: gas sensors for detection of heavy metals, adsorbents for treatment of waste water and contaminated soil, and photocatalyst for degrading of organic pollution.

2. Introduction of HAp

2.1 Structure of HAp crystal

There are various kinds of calcium phosphate (CaP) salts in nature and HAp is one of the most usual and thermodynamically stable phases of CaP salts. The crystal information of HAp is shown in Table 1. Each unit cell of stoichiometric HAp contains 10 Ca^{2+}, 6 PO_4^{3-} and 2 OH^-, among which OH^- ions are at 4 corners of the unit cell, 10 Ca^{2+} ions belong to two

different subsets Ca (1) and Ca (2). 4 Ca^{2+} ions occupy Ca (1) positions: two at z = 0, two at z = 1/2, which are at the center of the Ca-O octahedron consist of 6 O atoms. Other 6 Ca^{2+} ions occupy Ca (2) positions: three at z = 1/4 and three at z = 3/4, which are at the coordination center of three O atoms. 6 PO_4^{3-} tetrahedra are in a helical arrangement from levels z = 1/4 to z = 3/4. These PO_4^{3-} tetrahedra form the crystalline network of HAp and gives HAp structure its stability [10,11]. The structure information of HAp is shown in **Figure 1**.

Table 1: The crystal information of HAp [12,13]

Items	Information
Chemical name	Hydroxyapatite
Chemical formula	$Ca_{10}(PO_4)_6(OH)_2$
Ca/P ratio	1.67
Crystal system	Hexagonal
Space group	$P6_3/m$
Lattice parameters	a = b = 9.418 Å, c = 6.881 Å, β = 120°

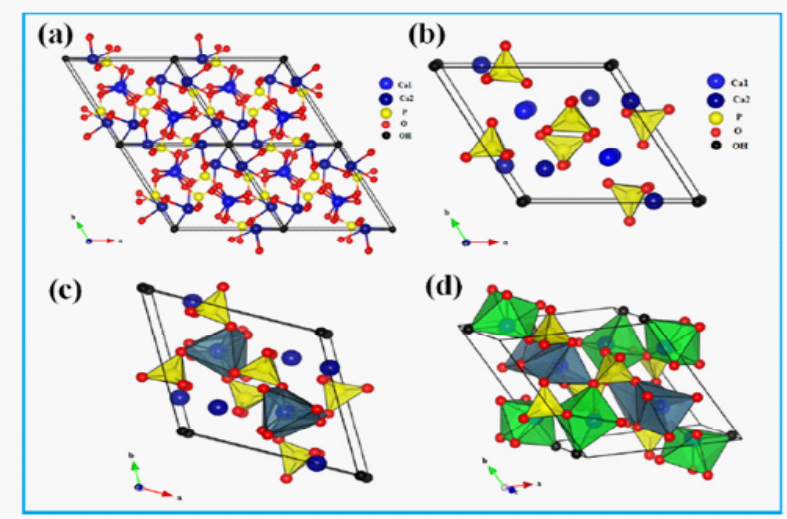

Figure 1(a): Projection of the unit cell of HAp according to plane (001); (b) projection showing the arrangement of octahedrons [$Ca(1)O_6$] in the HAp structure; (c) projection showing the sequence of octahedral [$Ca(1)O_6$] and tetrahedral [PO_4] in the HAp structure; and (d) projection showing the sequence of octahedral: [$Ca(1)O_6$] and [$Ca(2)O_6$] (green polyhedral), and also tetrahedral [PO_4] in the HAp structure [10].

When OH^- is at the side surface of the crystalline of HAp, OH^- is connected with 2 Ca (2) ions, this OH^- position must be vacant at least at a certain point in aqueous solution. The position of this OH^- can absorb PO_4^{3-}, phosphate groups of macromolecules or carboxyl groups since these 2 Ca (2) are positively charged. When Ca (1) is paralleled to the cross-section of HAp monocrystal, Ca (1) is connected with 6 negatively charged O atoms, in the meantime Ca (2) is connected with 3 negatively charged O atoms. In aqueous solution, the positions of Ca (1) are strong adsorption sites which can adsorb cations like Sr^{2+}, K^+ and groups of a protein molecules. In contrast, the positions of Ca (2) are weak adsorption sites. When PO_4^{3-} is on the surface of crystal, H_2O will bound to PO_4^{3-} by hydrogen bond.

www.openaccessebooks.com

2.2 Properties of HAp

The structure of HAp determines its properties. The theoretical density of HAp is 3.156 g/cm^3; the refractive index is 1.64~1.65; Moh's hardness is 5. HAp is only slightly soluble in water shows alkalescent (pH=7~9). At physiological pH (7.2-7.4), HAp is the most stable of all calcium orthophosphates [14]. HAp dissolves in acid but not dissolves in alkali.

2.3 Preparation methods of HAp

By varying the synthesis methods, HAp with different morphologies and properties can be obtained, which leads to different kinds of applications and performances. Synthetic pathways of HAp have attracted wide interest in academic research and industrial field. Over the past decades, numerous synthesis methods have been reported to prepare HAp nanoparticles. Generally speaking, dry methods and wet methods are the most often used synthesis methods. Each method has many process parameters, and the varying rage of conditions leads to many submethods. Several review articles about HAp preparation methods have been published [10,15,16]. Here just give a brief introduction to some mainly used methods.

As the name indicates, dry route of synthesis means there is no solvent in the reaction. Usually, the reactants are powders like $CaHPO_4$ and CaO, and these precursors are initially mixed and milled and then calcined at a very high temperature (around 1000 ℃) for quite a long time, which is its disadvantage [17-20]. After that, the outcome is a sintered bulk, therefore long-time milling or grinding process is needed in order to get nanoparticles. Another disadvantage is that the powders are always in irregular shape owing to the low diffusion coefficients of ions in solid state [21,22]. The main characteristic of dry methods is that the properties of synthesized powders are reproducible and homogeneous. Although there are many processing parameters, the product can be produced with conditions not precisely controlled. Thus, dry methods are suitable for industrial mass production of HAp. The most critical factor of the purity of HAp powder production is precise weighing procedures during preparation. Inaccurate weighing will lead to impurity or even different compositions such as other calcium phosphates.

In wet methods, the reactions are carried out in solutions at various temperatures. Comparing with dry methods, wet methods can be performed at various conditions: ambient temperature or high temperature, in water or in organic solutions, multiple reactants and apparatus to choose. The size of resultant powders is much smaller than dry methods, that is why researchers usually choose wet methods to synthesize nanoparticles. The morphology and the mean size of powder can be easily controlled. However, the crystallinity of HAp is lower than that of dry methods in many cases. Chemical precipitation may be the simplest method among wet methods. Besides, there are many other advantages including low reaction temperatures and environmentally friendly by-product (water). The typical procedure starts

with the preparation of the solutions containing Ca and P, and then dropwise add one reagent to another under continuous stirring. The molar ratio Ca/P has to be exactly kept at stoichiometry as 1.67. The precipitation is later washed, filtered, dried and heat-treated, respectively. Temperatures and pH can influence the morphologies of HAp powders.

Sol-gel methods are always used to produce fine powders in liquid medium. Generally, precursors undergo mineralization in aqueous. The process usually involves hydrolysis and polycondensation reactions which followed by drying on a hot plate and calcination. The conditions are really soft in terms of temperature, generally the highest temperature of the calcination is around 500 ℃, much lower than other methods [23]. However, shortcomings of this method are obvious: not suitable for industrial large-scale production, high expense, longer time expending, strictly controlling conditions.

Hydrothermal methods are one of the most common ways to produce HAp. The principle of these methods is similar to chemical precipitation, but the process usually occurs in a hydrothermal synthesis reactor with elevated temperature and high pressure, just like in an autoclave. The high pressure is the result of high temperature, which is much higher than the boiling point of water (sometimes the solvent is organic, which is called solvothermal). The HAp nanoparticles are relatively stoichiometric and highly crystalline. The morphology of HAp nanoparticles can be controlled by organic additives.

3. HAp as Gas Sensors for Detection of Environmental Gases

With the unprecedented development of industry, science and technology, industrial effluent and hazardous pollutant are emitted to the environment. The biosphere is badly hurt and many species are facing the threat of extinction. In order to prevent further impact of pollution, early detection of hazardous pollutant is critical for environmental security. Gas sensors play an important role in detecting specific gas molecules and environment protection. Thus, developing novel gas sensing materials becomes a hotspot. Owing to the unique properties of HAp, many researchers conducted related studies on its gas sensor applications. Here are introductions to some representative works.

3.1 Applications of HAp for detection of various gases

HAp has been applied to gas sensors for a long time. In 1988, Nagai *et. al.* [24] reported that porous HAp ceramics can be used as gas sensor for detecting CO_2, which is a common greenhouse gas. The fine HAp powders were prepared by conventional wet chemical method via the reaction between $CaCO_3$ and phosphoric acid. In 2005, Mahabole *et. al* .[25] developed a new type of HAp ceramic served as a CO gas sensor. CO is a hazardous gas which may cause people's death. They synthesized different HAp with different Ca/P ratios by three processes: wet chemical process, hydrothermal process and microwave process. The results showed that

the optimal operating temperature for using HAp as CO gas sensor was about 125 ℃ and at other temperatures the respond was merge. The sensitivity factor is about 0.8 when the concentration of CO is 900 ppm. In 2011, Khairnar *et. al.* [26] deposited the HAp thick film on insulating alumina substrate using screen printing technique for detecting CO. The HAp powder was prepared via wet chemical precipitation process. Then they used swift heavy ions (SHI) irradiation to modify the surface morphology and the gas sensing properties of HAp film. The working temperature to detect CO gas was 150 ℃ ~ 195 ℃. Gas response was improved upon SHI irradiation. When HAp grain had the least average size, it had the best gas sensing performance. Their group then reported that HAp thick films were doped with Co and Fe ions. The addition of metal ions and surface modification by SHI improved the sensing properties of HAp films to CO gas drastically [27].

Yong Liu's group has reported the sensing properties of HAp and HAp-based composites for detecting of ammonia gas that is a caustic and hazardous gas with a characteristic pungent smell. In 2015, Li *et. al*. [7] prepared tubular HAp powders by methods of cation exchange membrane-assisted electrochemical deposition. Ca and P solutions were added into two containers, respectively. A cation-exchange membrane (Nafion membrane) was fixed between the two containers. The conducted electrochemical deposition was for 1 h and the reaction lasted for 7 days. The tubular HAp was assembled by nano HAp crystals. Tubular HAp based NH_3 sensors exhibit 1.35-1.65 times of response value than the sensor based on rod-like HAp produced by hydrothermal method. Zhang *et. al.* [7] synthesized functionalized graphene/HAp composites. They first prepared and functionalized graphene oxide (GO) with the aid of polydopamine (PDA) which acted as a template and a reductant for graphite oxide. Then they used its solutions to synthesize hydroxyapatite/graphene (GR) hybrid materials via in situ synthesis (named cHAp/GR) and biomineralization (named bHAp/GR). The cHAp exhibited needle-like crystals while bHAp exhibited micro-spheres morphology. bHAp/GR composites showed a much higher response to ammonia than that of cHAp/GR due to its much finer crystals and nano-porous structures. In 2016, nano Au particles were also used by their group to improve the gas sensing properties of tube-like HAp [28]. 5wt% Au-modified HAp exhibited the best sensitivity and relatively short response/recovery time when detecting NH_3 gas. The response of the composite is still up to 70.8% when the NH_3 gas concentration is down to only 50×10^{-6}.

Except for metal ions and graphene, HAp can also be modified by conductive polymer. In 2016, Li *et al.* [29] prepared conductive polymer/HAp composite materials as the gas sensing materials to ammonia. HAp was prepared by cation exchange membrane-assisted electrochemical deposition. The composites were prepared by mechanical mixing of HAp powder with polyaniline (PAni) or polypyrrole (PPy). The results showed that both of PPy and PAni improved the sensing properties of HAp. Composites containing 5% PPy and 20% PAni

exhibited the highest sensitivity to NH_3. 5% PPy/HAp showed higher sensitivity and better selectivity than 20% PAni/HAp, but 20% PAni/HAp exhibited shorter response/recovery time and better stability.

Gram-negative bacterium was also be used to enhance the gas sensing properties of HAp by Liu's group, which is an innovative idea for material preparation. *Acidithiobacillus ferrooxidans* (*At.f*), is a Gram-negative bacterium, which can obtain energy through the electrons released as a consequence of the oxidation process and it is often used for desulphurization. In 2016, Tan *et. al*. [29] reported the results of *At. f*/HAp composites as gas sensing materials to detect H_2S gas. The sensitivity of the composite to H_2S was 2.5 times that of pure HAp. The highest sensitivity to H_2S at 2000 ppm was 76%. The microstructures are shown in **Figure 2**.

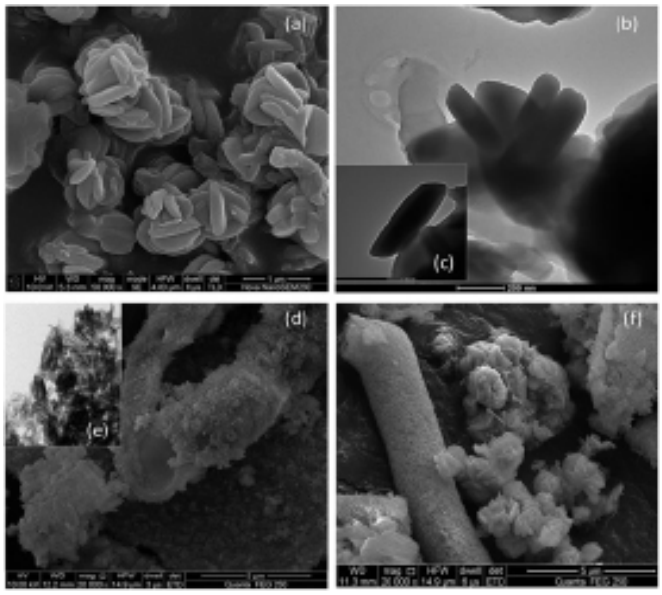

Figure 2: Microstructures of *At.f* (a–c), HAp (d and e) and *At.f*/HAp composite (f) [29].

3.2 Gas sensing mechanisms of pure HAp and the composites

3.2.1 Gas sensing mechanisms of pure Hap

HAp is known as a porous material with many ionic species like PO_4^{3-} , Ca^{2+}, and OH^-. HAp is usually recognized as a one-dimensional ionic conductor. OH^- is at the center of the channel which is paralleled to c-axis, Ca^{2+} is in the channel as well. The conductivity of HAp is generally recognized that protons serve as charge carriers and migrate from OH^- to the adjacent PO_4^{3-} in HAp crystals at room temperature [30]. When the temperature evaluates, OH^- will move along c-axis and that is the second conductivity mechanism of HAp. As mentioned above, porous structures greatly enhance the adsorption of HAp, the larger specific surface area is, the greater adsorption will be. Plus, the P-OH groups on the surface act as adsorption sites for gas molecules. HAp always acts as a proton acceptor. When the detected gas is CO, the reaction between CO molecule and OH^- on HAp surface is as following,

$$2OH^- + CO \rightarrow CO_2 + H_2O \quad (1)$$

$$2OH^- + CO_2 \rightarrow CO_3^{2-} + H_2O \quad (2)$$

The formation of CO_3^{2-} will have a great influence on the conductivity of HAp.

In Ref. [7], the tubular HAp grows preferentially along (002) orientation, *i.e,* c-axis. Since it is tube-like powder, the specific surface area is extremely large and the surface energy is pretty high. The crystallinity of tubular HAp is poorer than rod-like HAp, which lead to more defects of tubular HAp crystal. The more defects and larger specific surface area, the more absorption sites there will be. The absorption sites will absorb O_2 molecules and react as following,

$$O_2(gas) \leftrightarrow O_2(ads) \quad (3)$$

$$O_2(ads) + ne^- \leftrightarrow m(O_2^- / O^- / O^{2-}) \quad (4)$$

When NH_3 molecules are captured by absorption sites, they will act as a proton donor and produce intermediates of NH_2^- which will react with O_2^-, O^- and O^{2-}. HAp as a proton acceptor, its conductivity will increase owing to the increment of charge carrier. Besides, NH_2^- will probably replace OH^- on the surface, which will change the crystal structure of HAp. That may be another reason of conductivity change.

$$NH_3 \leftrightarrow NH_2^- + H^+ \quad (5)$$

$$NH_2^- + (O_2^- / O^- / O^{2-}) \leftrightarrow NO_x^{n-} + H_2O \quad (6)$$

HAp can also absorb H_2O, as is known to all, NH_3 is highly soluble in water and can produce NH_4^+, the conductivity will increase.

The schematic illustration of ammonia sensing mechanisms of tubular hydroxyapatite is shown in **Figure 3**.

$$NH_{3(g)} + H_2O \xleftrightarrow{RT} NH_{4(ads)}^+ + OH_{(ads)}^- \quad (7)$$

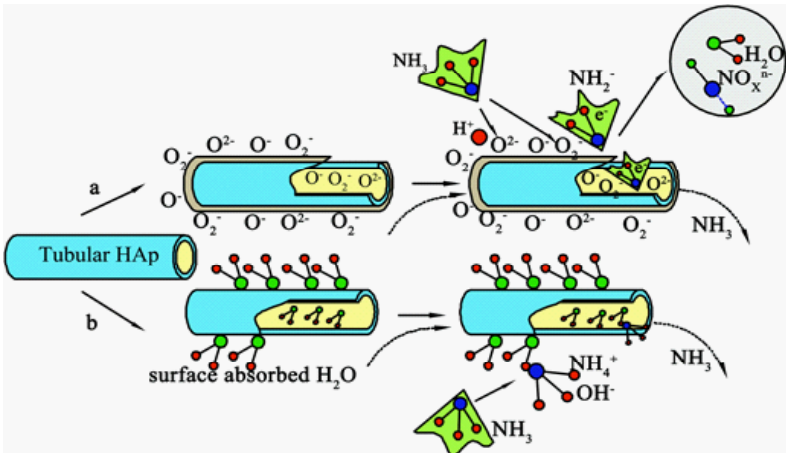

Figure 3: Schematic illustration of major ammonia sensing mechanisms of tubular HAp [7].

3.2.2 Gas sensing mechanisms of HAp based composites

The mechanism of HAp based composites varies a lot according to the component. For two-dimensional materials like graphene, HAp acted as an anchor and absorb gas molecules, and GR is a good conductor, this combination can perfectly enhance the gas sensing properties. For metal ions, besides its great conductivity, the catalysis effect also plays an important role. The surface of gold nanoparticles carries negative charge, so it has strong ability to capture NH_3 molecules. As a catalytic activator, Au nanoparticles result in more defects on the surface of HAp, which increase the sensing ability of composites [28]. For polymers like PPy and PAni mentioned above, PPy is a p-type semiconductor, its carrier is a positively charged vacancy, and ammonia, as a reducing gas, contributes electrons to PPy. When the concentration of charge carrier of PPy decreases, the resistance increases. When the concentration of NH_3 goes up, the number of molecules adsorbed by PPy goes up, thus improving its sensitivity [29].

As for bacterium, the cell wall of *At.f* is composed of many kinds of polysaccharides and proteins, which means there will be many chemical activate groups like hydroxyl, carboxyl and mer\capto-group. Moreover, when H_2S is absorbed by H_2O, H_2S will dissociate to HS^- and H^+, which increases the density of proton, so the conductivity will increase when the concentration of H_2S increases. Another reason for the improvement of the sensitivity is that during the cultivation of *At.f*, jarosite ($KFe_3(SO_4)_2(OH)_6$) was formed, which has been used as a catalyst. The multiple OH^- groups in jarosite can provide the adsorption sites for H_2S. In addition, Fe^{3+} and SO_4^{2-} in jarosite may also be beneficial for the response to H_2S since they may provide the selective oxidation of hydrogen sulfide to sulfur [29].

4. Electrochemical Detection Of Heavy Metals and other Organics By Hap

With the rapid development of China's industrialization, the situation of water and soil pollution have become increasingly serious. Excessive levels of heavy metals in human body have become more and more common. The harm caused by heavy metals to human health cannot be ignored, such as lead poisoning and Minamata disease. These poisoning symptoms often bring serious permanent damages to human body, leading to disability and even death. Metals with a density of more than $4.5g/cm^3$ are often called heavy metals, such as gold, silver, copper, lead, zinc, nickel, cobalt, chromium, mercury, cadmium and so on. In terms of environmental pollution, heavy metals refer to the elements with significant biological toxicity, such as chromium, mercury, cadmium, lead and arsenic, which are also the most five toxic heavy metals to human body. They cannot be decomposed in water, and their toxicity will be amplified after drinking by mistake, and they can combine with other toxins in water to form more toxic organic or inorganic substances. **Table 2** summarizes the hazardness of some heavy metals mentioned above.

Table 2: Examples of some heavy metals reported in the literature.

Metal	WHO standard limits(mg/L)	Main sources	Poisoning effects	References
Lead (Pb)	0.05	PVC pipes in sanitation, agriculture, recycled PVC lead batteries, lunch boxes, etc.	Penetrates through protective Blood Brain Barrier (BBB) and is proving to be a risk factor for Alzheimer's disease and Senile Dementia. Also leads to neuro-degenerative diseases, decreases IQ, kidney damage, decreased bone growth, behavioural issues, ataxia, hyperirritability, and stupor	[24, 25, 27, 31, 32]
Cadmium (Cd)	0.005	Paints, pigments, electroplated parts, batteries, plastics, synthetic rubber, photographic and engraving process, photoconductors and photovoltaic cells	Renal toxicity, hypertension, weight loss, fatigue, microcytic hypochromic anaemia, lymphocytosis, pulmonary fibrosis, atherosclerosis, peripheral neuropathy, lung cancer, osteomalacia, osteoporosis, and hyperuricemia	[33-35]
Arsenic (As)	0.05	Wooden electricity poles that are treated with arsenic based preservatives, pesticides, fertilizers, release of untreated effluents, oxidation of pyrite (FeS) and arseno pyrite (FeAsS)	Causes effects on central nervous system (CNS), peripheral nervous system (PNS), cardiovascular, pulmonary diseases, gastrointestinal tract (GI), genitourinary (GU), haemopoietic, dermatologic, foetal and teratogenic diseases, anorexia, brown pigmentation, hyper-pigmentation, localized edema, and skin cancer	[36-39]
Chromium (Cr)	0.05	Leather industry, tanning, and chrome plating industries	Reproductive toxicity, embryotoxicity, teratogenicity, mutagenicity, carcinogenicity, lung cancer, dermatitis, skin ulcers, perforation of septum, and irritant contact dermatitis	[40]
Zinc (Zn)	5	Soldering, cosmetics, and pigments	Respiratory disorders, metal fume fever, bronchiolar leukocytes, neuronal disorder, prostate cancer risks, macular degeneration, and impotence	[41-44]
Copper (Cu)	1.3	Fertilizers, tanning, and photovoltaic cells	Adreno-corticol hyperactivity, allergies, anaemia, alopecia, arthritis, autism, cystic fibrosis, diabetes, haemorrhage, and kidney disorders	[45, 46]

4.1 Introduction of detection methods

The content limit of hazardous heavy metals is extremely low to human health, regular method is not easy to detect them and once detected, severe complications have been caused. So, a detection method with high sensitivity, better accuracy and faster response speed is required. The following will introduce two kinds of commonly used electrochemical detection methods for determination of heavy metals: anodic stripping voltammetry and cathodic stripping voltammetry.

4.1.1 Anodic stripping voltammetry (ASV)

A standard analytical electrochemistry system mainly consists of three parts: an electrochemical sensing device, electrochemical detecting instrument, and electrolyte. The electrochemical detection instrument is usually composed of three electrodes: a working electrode (WE), reference electrode (RE), and counter electrode (CE). After the surfaces of the WEs are modified using different materials, WEs have a uniform surface area and maintain sensitive response and they can be used for the specific detection of various kinds of metal ions [47, 48].

Stripping voltammetry includes two steps: pre-concentration and dissolution. The pre-concentration step involves accumulating the metal cations on the surface of the WE using Faraday's reaction or adsorption, and then obtaining a correlated signal by anodic stripping voltammetry (ASV). Following the pre-concentration step, the dissolution step is carried out by sweeping the electrode potential in the anodic direction to re-oxidize the zero-valent metals to cations [49]. A high dissolution current peak is reached during the rapid oxidation process, and the stripping current peak potential changes according to the different kinds of heavy metals.

Square wave anodic stripping voltammetry (SWASV) is one of the common and typical means of ASV. It has numerous applications in various fields, including medicinal and various sensing detection. SWASV measurement also includes two steps: accumulation of trace elements and electrochemical stripping step of the accumulated elements on electrode surfaces [49]. Considering the two steps of SWASV, it is very important to select a suitable material which is easy for adsorption and stripping of heavy metal ions to modify the surface of working electrode for sensitively electrochemical detection. Recently, the researchers are exploring electrode materials that can promote the oxidation-reduction reaction between an electrode and metal ions. For example, Li and Zhang used an ionic liquid supported CeO_2 nanoparticles–carbon nanotubes composite modified glassy carbon electrode as an electrochemical sensor to detect Pb^{2+} [50].

4.1.2 Cathodic stripping voltammetry (CSV)

Stripping voltammetry is also known as reverse stripping polarography. This method allows the substance to be measured to electrolyze for a certain time under the potential of limiting current generated by ion polarography analysis. Then the potential of the electrode is changed so that the substances concentrated on the electrode can be dissolved out again. The voltammetry curves obtained in the dissolution process are used for quantitative analysis. If the cathode is used for dissolution reaction, it is called cathodic stripping voltammetry (CSV). In this method, the measured ions form a layer of insoluble compounds in the anode process of pre-electrolysis, and then when the working electrode is scanned in a negative direction,

the insoluble compounds are reduced and a reduction current peak is generated. CSV can be used for the determination of anions such as halogen, sulfur and tungstate [51,52].When it is used to detect metal ions, the enrichment effect is independent of the initial concentration. In order to achieve a good enrichment effect, the concentration time can be shortened by reducing the solution volume, increasing the area of the electrode, speeding up the mixing speed and reducing the thickness of the diffusion layer [53]. Because of the high sensitivity of stripping voltammetry, it has practical value in the analysis of ultrapure substances. In addition, it has been widely used in the determination of trace elements in environmental monitoring, food, biological samples and so on.

4.2 Detection of heavy metals and other organics by HAp

4.2.1 Detection of heavy metals and other organics by pure Hap

Effective remediation of heavy metal contaminated wastewaters is one fundamental step towards a more sustainable industrial development. The detection process, due to its simplicity has attracted a lot of interest. Activated carbons have been the most popular and widely used materials [54-57], however, the high costs have limited their diffusion on an industrial scale.

Among all the solid detection agents and sorbents, HAp has gained a major attention because of its unique properties of low cost, chemical and thermal stability, and extreme water insolubility (Kps $\approx 10^{-59}$ at room temperature) [58]. The HAp structure is flexible to both cationic and anionic substitutions, which yields the possibility of functionalizing the structure and modulating the number of acid–base sites in the HAp crystal. Cations (e.g., Sr^{2+}, Mg^{2+}, Na^{+}, K^{+}, etc.) can substitute either Ca(1) or Ca(2) ions or both simultaneously, whereas anions (e.g., F^{-}, Cl^{-}, CO_3^{2-}, VO_4^{3-}, etc.) can replace either OH^{-} or PO_4^{3-} ions or both simultaneously [59-63].

It has been proved that HAp is an effective detection agents and adsorbent for various metal cations [64-68]. More than one metal-trapping mechanism has been recognized: ion-exchange that involves the substitution of Ca^{2+} ions of the HAp framework, surface complexation, and dissolution-precipitation of new formed stable phosphate containing phases [47,64,67,68]. The predominance of a certain metal trapping mechanism depends on the metal species nature, the operative parameters, such as pH and contact time, and also the surface characteristics (acid-base sites ratio) of HAp sample [68]. From an applicative point of view, HAp presents the advantage that mono-valent, bivalent, trivalent, and even higher valence metal ions can partly or completely substitute Ca^{2+} ions of HAp framework. If the substituting cation does not have a +2 charge, the charge compensation mechanism might have an overriding influence on the distribution between the Ca(1) and Ca(2) sites. So, there may be an unequal distribution of substituting cations between them. If the cation substitution does not imply charge difference, the distribution is more likely to be determined by the relative sizes of the substituting and host

cations in relation to the two Ca sites, although the polarizability and the ability to form partial covalent bonds may be important in particular cases. The coordination number of the Ca(1) site is nine, whereas for Ca(2), it is only seven. This difference can suggest that, purely on the basis of the size, the Ca(1) site should be occupied preferentially by cations larger than Ca(1) (e.g., effective ionic radius for several ions in the same coordination, VI-coordination, Ca^{2+}, Sr^{2+}, Pb^{2+}, and Ba^{2+} are 1.00, 1.18, 1.19, and 1.35 Å, respectively). Moreover, an important advantage of HAp sorbent is the almost permanent character of the confinement of several trapped metal species [65,68].

In 2011, Zhang, *et al* [36] have successfully converted waste egg-shell to HAp under hydrothermal conditions, and applied it as modifiers in chemically modified carbon paste electrode (CMCPE) for highly sensitive detection of bisphenol A(BPA) in 0.2M phosphate buffer saline(PBS) by cyclic voltammetry method. HAp modified electrode exhibited excellent sensing ability, with the detection limit down to 0.246 nM in a linear range of 0.4 nM to 24nM. They [69] also have successfully converted the egg-shell to 3D flower-like HAp under mild conditions, and applied it as modifier in electrochemical sensor for the detection of As^{3+} by cyclic voltammetry method. It exhibited excellent sensing ability with the detection limit down to 0.034 ppb [69]. They also used the flower-like HAp crystals formed on the egg-shell membrane as modifiers in CMCPE for highly-sensitive detection of Pb^{2+} and Cd^{2+} ions by ASV method [70]. The results revealed that the HAp exhibits better adsorption ability than brushite because of its unique three-dimensional network structure as well as the high flexibility in ion exchange. The change of crystal lattice structure leads to the difference of determination capability for metal ions. The detection limits of CMCPE modified by HAp achieved 2.38nM for Pb^{2+} and 5.31nM for Cd^{2+} in a linear range of 1.0nM to 100nM [70]. Zhang, *et al* [71] also fabricated sea cucumber-like HAp crystals with the aid of a Nafion N-117 cation exchange membrane and the crystals were used as modifiers in a CMCPE for the detection of Pb^{2+} and Cd^{2+} ions by SWASV method. The SEM images of HAp crystals are shown in Fig. 4. The unique sea cucumber-like HAp exhibited better adsorption ability than HAp nanorods. The proposed modified electrode had significantly lower linear ranges for Pb^{2+} and Cd^{2+} with a detection limit of 0.00423nM and 0.027nM, respectively, and exhibited sensitivities about 10 and 100 times higher than those reported previously for other HAp–CPEs.

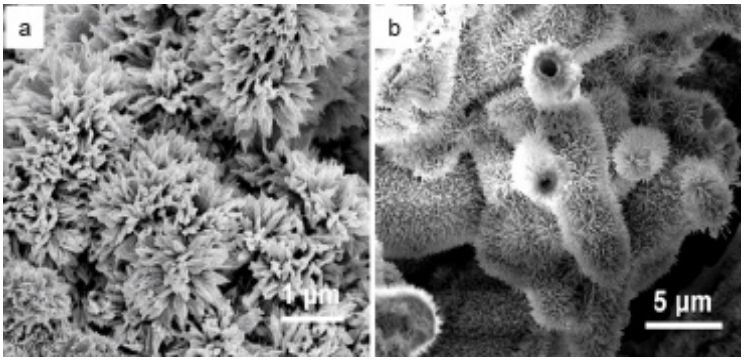

Figure 4: Morphologies of the crystals formed on the P-side of the cation exchange membrane after holding for (a) 4 days and (b) 7 days.

4.2.2 Detection of heavy metals and other organics by HAp-hybrid materials

Synthetic HAp is an efficient and environment-friendly material for the remediation of heavy metal contamination. However, the applications of conventional HAp powder in stabilizing pollutants are limited, due to the lower performance/price ratio. Therefore, more and more attentions are put on the HAp-hybrid materials to combine the both advantages of HAp and additive agents. Prongmanee *et. al.* [72] prepared HAp/ GO composites by growth of HAp on GO in the simulated body fluid (SBF). HAp/GO modified screen-printed electrode (SP-HAp/GO) were investigated for L-tryptophan (Trp) detection using linear sweep voltammetry (LSV) technique. After electrochemical determination of Trp, the linear range (7–1,000 µM) and limit of detection (LOD ~ 5.5 µM) obtained from HAp/GO-modified electrode are better than those of bare (25–1000 µM, LOD ~ 17.5 µM) and GO-modified (10–1000 µM, LOD ~ 7.0 µM) electrode. Pang, *et. al.* [73] used a simple and sensitive electro chemical method for the determination of luteolin based on the graphene nanosheets (GNs) and HAp nanocomposite modified glassy carbon electrode (GCE) (GNs/HAp/GCE). The electrochemical behaviors of GNs/HAp/GCE can greatly enhance the electrocatalytic activity in the redox process of luteolin. It led to a considerable improvement of the redox peak current for luteolin and allowed the development of a sensitive voltammetry sensor for the determination of luteolin. The results showed that the detection limit was 1.0×10^{-8} M. Ajab *et. al.* [74] synthesized an environmentally friendly and cost-effective novel carbon electrode modified with cellulose and HAp to detect Pb ions. The sensor detected Pb ions in palm oil mill effluent in the concentration range of 10–50 µg/L with 0.11 ± 0.37 µg/L limit of detection and 0.37 ± 0.37 µg/L limit of quantification. They also synthesized a novel cellulose, HAp and chemically-modified carbon electrode (Cellulose-HAp-CME) composite for the detection of trace Pb^{2+} and validation in blood serum by SWASV(75), with LOD of 0.11 ± 0.36 ppb and limit of quantification (LOQ) of 0.36 ± 0.36 ppb.

Table 3 shows the summary of the applications of HAp on detection of heavy metals and other organics.

Table 3: Detection of heavy metals and other organics by HAp and its composites

Materials	Synthetic approach	Morphology	Template/ surfactant	Application	Reference
HAp	hydrothermal	Flower-like	Egg shell	Detection of bisphenol A	[36]
HAp	/	3D flower-like	Egg shell	Detection of As^{3+}	[69]
HAp	Ion exchange	Flower-like	Egg shell membrane	Detection of Pb^{2+}, Cd^{2+}	[70]
HAp	Ion exchange	Sea cucumber-like	Nafion membrane	Detection of Pb^{2+}, Cd^{2+}	[71]
SP-HAp/GO	/	/	SBF	Detection of L-tryptophan (Trp)	[72]
GNs/HAp/GCE	Electrochemical method	/	/	Detection of luteolin	[73]
Cellulose-HAp-CME	/	/	/	Detection of Pb^{2+}	[74, 75]

4.3 Section summary

To sum up, HAp and its composites are functional materials for the efficient detection of heavy metals and other organics in wastewater. The future studies can be carried out in the following aspects: (1) The application of HAp is limited due to its powder structure. Therefore, in order to improve the performance and practicability, HAp can be combined with organic or inorganic materials to form a practical composite detection material. (2) At present, the proposed mechanisms of detecting heavy metals by HAp include ion exchange, surface complexation, adsorption and dissolution/precipitation. However, there is still a lack of in-depth theoretical and experimental support for the specific determinative effects.

5. Adsorption of heavy metals by Hap

Water and soil contamination by heavy metals has become a major global concern and represents a significant threat to the environment and human beings. Unlike most organic contaminants, the major concern regarding the presence of heavy metals in an environment is that such metals have direct or indirect adverse effects on animals, plants and humans, even at very low concentrations. Due to their non-biodegradability and long-term persistence, which result in their accumulation in living organisms and concentration throughout the food chain, they can cause severe environmental contamination, as well as various diseases and disorders [76,77], which is shown in **Table 2**.

Adsorption is one of the attractive methods for the removal of metal ions or organic contaminant in aqueous environment in terms of simplicity, suitability for ultra-low concentration, and availability of different low-cost adsorbents. Along with the need of low-cost

adsorbent, many inorganic and organic materials were developed for waste water treatment and soil remediation. Instead of carbon-based materials such as biochar, bio-sorbent and activated carbon, HAp were also widely studied [78, 79]. HAp has been reported as a suitable material for the removal of heavy metals from contaminated water and soil [10,80-82]. This is due to the physical, chemical, mechanical and biological properties that make it stable and exhibiting high sorption capability. These properties are related to various surface characteristics of HAp, e.g., surface morphology, surface functional groups, acidity and basicity, surface charge, hydrophilicity, and porosity [83-85].

5.1 Adsorption of heavy metals from water by HAp

Studies on the adsorption of heavy metals by HAp began at the end of the 20th century. In 1994, Suzuki, *et. al.* [86] applied the fixed bed containing HAp particles as the adsorption material of Cu^{2+}, Cd^{2+} and Pb^{2+}. It was found that the adsorption of Cd^{2+} and Cu^{2+} was mainly on the surface of HAp particles, and Pb^{2+} could be adsorbed inside and outside the particles. In 1996, *Reichert, et. al.* [87]. developed three HAp based adsorption materials for the removal of Cr^{3+}, Pb^{2+} in water. The results showed that the removal rate reached 100%. After 2000, researchers conducted further studies on HAp for removal of heavy metals.

Skwarek, *et. al*. have prepared and modified HAp, and studied the adsorption capability of some metal ions on HAp/electrolyte solution, including Zn^{2+} [88], Sr^{2+} [89,90], Cd^{2+} [91], Co^{2+} [92], Ba^{2+} [93] and U^{6+} [94] ions. Adsorption of Zn and Sr ions in the studied pH range and can be described using the Freundlich equation [88, 89], which means the adsorption sites on the surface were heterogeneous. The adsorption kinetics of Sr, Cd, Co, and Ba ions can be described by the multiexponential equation. The adsorption kinetics of U ions followed the pseudo-second-order model. The solubility/dissolution and precipitation process that occurred during the adsorption of Sr and Cd ions due to H^+ release, which then changed the grain or particle size distribution of HAp [89,91]. Metals ions removal from aqueous solutions by HAp can proceed through different sorption processes, such as ion-exchange, surface complexation, coprecipitation, recrystallization, contigent on the applicaiton conditions and feature of both sorbing cations and HAp [89]. For Co ions adsorption, it proceeds by ion-exchange with Ca ions in the crystal lattice and H ions in the surface groups of HAp [92]; for Ba ions adsorption, it occurs by their adsorption of ions on the surface groups with the release of proton and the exchange of Ca ions from the crystal lattice [93]; for U(VI) ions adsorption, it proceeds as the chemisorption mechanism [94].

Bitter gourd is a well-known vegetable with many holes on the surface. Guo. *et al* [95] synthesized an interesting bitter gourd-shaped nanoscale HAp (**Figure 5**), with a high adsorption capacity of heavy metal ions (Pb^{2+}, Cd^{2+}, Cr^{3+}). The adsorption capacity for Pb^{2+}, Cd^{2+}, Cr^{3+} is 815.4, 291.5 and 187.3 mg/g, respectively. The main interaction mechanism may

possibly be ion-exchange mechanism. But different from the reported ion-exchange mechanism in which the main exchange ions is H^+ [96-99], the exchange ions of the bitter gourd-shaped nano-HA is Ca^{2+}.

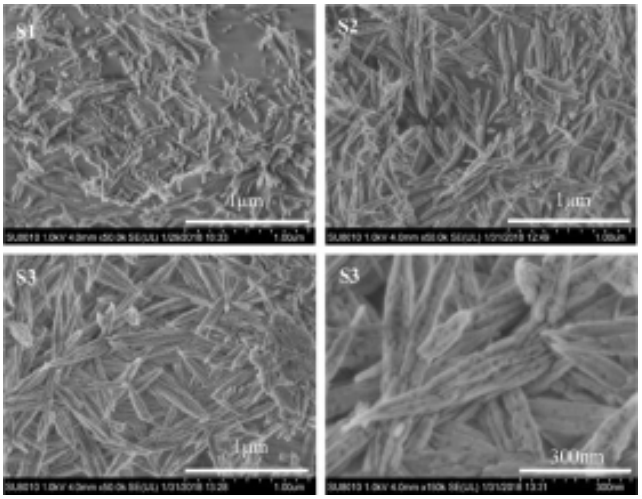

Figure 5: SEM images of bitter gourd-shaped nanoscale HAp [95].

Biochar (biomass-derived black carbon) has attracted attention as a new adsorbent because of its especial properties (e.g., high surface area and cation exchange capacity) [100-102]. However, the as-prepared biochars usually have a relatively low adsorption capacity for heavy metals [103]. A HAp-biochar (HAp-BC) nanocomposite was synthesized and used for Pb^{2+}, Cu^{2+} and Zn^{2+} removal in both single and ternary mixed solutions [104]. The HAp-BC nanocomposite showed enhanced adsorption, especially for Pb^{2+}. The adsorption capacities of HAP-BC are higher than those by BC. Pb^{2+} adsorption followed the Langmuir model, while the other two ions followed the Freundlich model in both single and ternary systems. All adsorption processes were well-described by pseudo-second-order kinetics. In addition, the adsorbed HAp-BC could be recycled using HCl solution. Thus, HAp-BC nanocomposites could be an eco-friendly and low-cost adsorbent for heavy metals removal from wastewater.

Generally, the adsorbent should be environmentally friendly and causes no secondary pollution. However, the aggregation of nano-HAp in aqueous solutions without stabilizers will lose removal capacity. Moreover, well-dispersed and highly stable nano-HAp is not easy to be isolated from aqueous solutions after usage. So, the nano-HAp suspension was synthesized with the stabilization effect of polyacrylic acid and further fixed by alginate to form nano-HAp/alginate composite for Cu^{2+} removal, showing adsorption capacity is 60.99 mg/g for Cu^{2+} [105]. For nano-HAp, the Langmuir isotherm model was more suitable to describe the adsorption of Cu^{2+} ions. For 50% nano-HAp/alginate composite, the adsorption of Cu^{2+} followed both the Langmuir and Freundlich isotherm models. That is to say, the multilayer adsorption of Cu^{2+} may occur on heterogeneous surface of nano-HAp/alginate composite compared to the monolayer sorption of Cu^{2+} onto nano-Hap [106].

Higher rates in metals removal can be obtained when the solid matrixes employed are

not used only as immobilization surfaces but also play an active role in the adsorption of the metallic ions. Activated carbon, for instance, was employed with several bacteria on its surface, such as *Escherichia coli*, *Streptococcus equisimilis* and *Bacillus coagulans*, for the removal of Pb, Cd and Cr [107]. Piccirillo, *et. al.* [108] reported a study on the immobilization of metal-resistant bacterial strains onto the surface of HAp that was extracted from the bones of Atlantic cod fish for the removal of Zn^{2+} or/and Cd^{2+}. The synergistic effect between bacteria and HAp was effective for higher concentrations of heavy metals when removal one kind of metal ions, and for lower concentrations when more than one metallic ion is present in solution. The maximum adsorption capacities were up to almost 4 and 3 times higher for Zn^{2+} with 1C2 (*Cupriavidus sp.*) and Cd^{2+} with EC29 (*M. oxydans*) respectively. These systems were also tested for solutions containing both of these two metallic ions at the same time, and were shown to be effective also in these cases [109]. Some applications of HAp for adsorption of heavy metals are summarized in **Table 4**.

Table 4: Adsorption of heavy metals by HAp and its composites

Materials	Adsorption heavy metals	Saturation absorptive capacity(mg/g)	Adsorption mechanism	Reference
Ag-HAp, Ca-HAp	U^{6+}	8.1 mmol/g for Ca-HAp; 7.2 mmol/g for Ag-HAp	Chemisorption	[94]
Bitter gourd shaped HAp	Pb^{2+}, Cd^{2+}, Cr^{3+}	for Pb^{2+}, Cd^{2+}, Cr^{3+} is 815.4,291.5 and 187.3,	Ion exchange (Ca^{2+})	[95]
HAp-BC	Pb^{2+}, Cu^{2+}, and Zn^{2+}	maximum adsorption values for Pb^{2+}, Cu^{2+}, and Zn^{2+} were about 1000, 833.33, and 935.	adsorption/desorption cycles	[104]
nano-HAp/alginate composite	Cu^{2+}	60.99	Dissolution-precipitation, ionic exchange reaction and surface complexation	[105]
HAp(bacteria: Cupriavidus sp. And M. oxydans)	Zn^{2+}, Cd^{2+}	Zn^{2+}:0.433 mmol/g Cd^{2+}:0.090mmol/g	Synergistic effect between HAp and the bacterial	[108]

5.2 Adsorption of heavy metals from soil by HAp

HAp has been used for soil remediation because of its adsorption and immobilization ability of heavy metals. In 1999, Boisson, *et. al*. [110] evaluated the possibility of HAp as a metal immobilizing additive for soil remediation. It showed that concentrations of metals in the leaves of the test plants reduced after HA application. Several researches [111-114] have proved that HAp is a potential material for Pb and Cd contaminated soil remediation. Wang *et. al*. [115] used composite agents containing KCl and HAp for soil remediation contaminated by Pb and Cd. The results showed that HAp could fix the Pb and Cd efficiently, with a maximum fixing efficiency of Pb and Cd for two types of soil were 83.3%, 97.27% and 35.96%, 57.82%, respectively. Cl^- improved the fixing efficiency of Pb/Cd in soil by HAp. He *et.al.* [116] prepared a nano-crystallite HAp to immobilize Pb and Cd in contaminated

soil. The nano-HAp application could significantly reduce water soluble Pb with 72% and Cd with 90%, bioaccessible Pb with a reduction of 12.5-27.5% and Cd with a reduction of 17.66-34.64%, respectively. The phytoavailability of Pb and Cd was reduced with 65.3% and 64.6% in contaminated soil, respectively. Yang, *et.al.* [117] used a biochar-supported nano-HAp (nHAp@BC) for remediation of Pb contaminated soil. Using BC can greatly reduce the cost of remediation of Pb though it reduced the immobilization rates of Pb. Moreover, nHAP@BC can reduce the bioaccessibility of Pb in the soil and the accumulation of Pb in plants, and accelerate the recovery of soil fertility. Li, *et.al.* [82] studied the influence of particle size of HAp on the efficiency of soil remediation. They found that micrometer HAp (mHAp) is more effective than nanometer HAp (nHAp) on remediation multiple metal-contaminated soils and was more suitable to be applied in in situ remediation technology. Another group [118] also studied the influence of particle size and surface characteristics of HAp particles on the soil remediation effect and obtained the similar results. MHAp had better effect on the passivation of plant available heavy metals in soil, while NHAp had better passivation durability. Wang *et.al.* [113] studied the adsorption behavior and fixation effects of HAp on Pb contaminated soil, and discussed the mechanisms for soil remediation by HAp. According to the results, the adsorption of Pb^{2+} by HAP was a monolayer adsorption, and the main adsorption process was mainly dominated by surface reactions and chemical reactions. They concluded that the ion exchange, phosphorus supply, precipitate, and complexation are the main immobilization mechanisms for soil remediation with HAp.

5.3 Section summary

In conclusion, HAp and its composites are functional materials that can effectively remove heavy metals from water and soil. Further studies can be carried out in the following aspects: (1) The studies on the mechanism of HAp adsorption of heavy metal ions should be strengthened. At present, the adsorption mechanism of HAp surface is tentative and still stays on specific materials. The adsorption behavior of HAp can be guided by improving existing models or developing new general theoretical models with better practicability. HAp desorption behavior after adsorption of heavy metal ions still need to be studied. (2) HAp modification needs to be studied to make its surface structure be more suitable for practical needs, so as to simplify the production process, reduce the preparation cost. Also, HAp powder needs to be more refine, homogeneous, activation to improve the removal rate of heavy metal ions with less adsorbent and improve the conditions of adsorption (excellent stripping and recycling properties).

6. Photocatalytic Degradation of Hazardous Substances

Organic dye pollutants are ubiquitous water contaminants because of their widespread applications in industry [119]. These compounds can not only alter the electrical conductivities

of bio-membranes and inhibit cellular enzymes but also produce mutations in animal (including human) cells and exhibit teratogenic, carcinogenic, and reproductive effects [120]. Moreover, due to their intrinsic biological activity, their partial or complete degradation prior to discharge is needed [121]. With this purpose, ozonation and other advanced oxidation technologies have been developed [122,123], among which photodegradation appears particularly promising [124]. This technology relies on the use of a photocatalytic material, in most cases a nanoscale semiconductor, and can generate highly oxidative species under light excitation [125]. While titanium dioxide remains the most popular photocatalyst used for pharmaceuticals photodegradation [126], ZnO, Fe_2O_3, Ag_3PO_4, Pt and so on have also shown interesting potentialities in this field [127].

Among absorbing phases that may be advantageously associated with ZnO, HAp appears particularly interesting due to its high capacity for metal ions retention and good adsorption properties towards certain organic pollutants, including antibiotics [128-132]. The co-precipitation of HAp-based nanocomposites with other inorganic phases, such as ZrO_2, Fe_3O_4 or TiO_2, for remediation purpose has already been reported [133,134]. In particular, Ti-doped HAp have shown very promising properties as photocatalysts [135-138].

6.1 Photocatalytic degradation of hazardous materials by HAp composites

Organic dyes widely exist in the effluent from paper and textile industrial wastewater and can cause serious environmental problems and damages to human health [139, 140]. The oxides with photocatalytic function and HAp with excellent adsorption property were compounded at the atomic level. In other words, part of Ca in HAp was replaced by metal atoms in metal oxides to form a structure similar to that of photocatalytic oxides at the place where the metal atoms were replaced. That is to say, the photocatalytic function is given to the HAp crystal structure with excellent adsorption property, so that the decomposed object can be oxidized and decomposed efficiently. Recently, doping different ions in apatite lattice has been proved to be an effective way to enhance the photocatalytic efficiency of HAp. For example, Nishikawa, *et. al* .[141] firstly revealed that after substitution of a part of Ca ions by V ions in HAp lattice (V:HAp), visible light driven photocatalytic activity of HAp appeared. The substituted V ions were pentavalent at bivalent Ca sites, causing the introduction of amounts of Ca defects in the HAp lattice to keep electric neutrality. The photocatalytic activity was increased with V content. The V ions in the HAp lattice seemed to play a role as electron acceptor and the redox potential of the level due to the V ions was negative enough to reduce a O_2 molecule into H_2O_2 via two-electron process.

Visible-light-driven photocatalysts have received much attention in the current situation of energy shortage and environmental remediation(142). Liu, *et. al.* [143] explored a visible-light-driven amorphous photocatalyst made from amorphous Fe (III)-substituted hydroxyapatite

(am-Fe-HAp) by low cost ion-exchange method. The am-Fe-HAp with large surface area had semiconductor property and exhibited a good photocatalytic activity for the degradation of a smart ink and rhodamine B (RhB) under visible light. The photocatalytic effect of am-Fe-HAp could be attributed to the impurity energy level induced by the doped Fe^{3+} ions. The electrons from the impurity energy level could be excited into the conduction band of am-Fe-HAp, which resulted in the semiconductor property under visible light.

TiO_2 is the most commonly used and extensively investigated photocatalyst due to its low cost, non-toxicity, favorable band edge positions, high catalytic efficiency and chemical stability [144]. Singh, *et. al*. [145] used low-cost waste mutton bone to prepare HAp and then incorporated it with TiO_2 nanoparticles (HAp-T) by simple sol-gel route. HAp-T nanoparticles demonstrated efficient degradation of the methylene blue (MB) dye (~93%) under UV irradiation. Besides, appreciable stability and reusability attributes of HAp-T nanoparticles were observed for over 10 cycles of reuse (**Figure 6**(**a**)). Crystal structure and morphology of HAp-T nanoparticles photocatalyst did not alter significantly after 10 cycles of reuse (**Figure 6** (**b**)). During the degradation process, HAp support can adsorb the MB molecules due to its excellent adsorptive nature and improve the reaction probability between MB molecules and excitons. HAp support contributed to recovery of photocatalyst after every reuse, which guaranteed its long-term stability, and also restrained the agglomeration of TiO_2 nanoparticles.

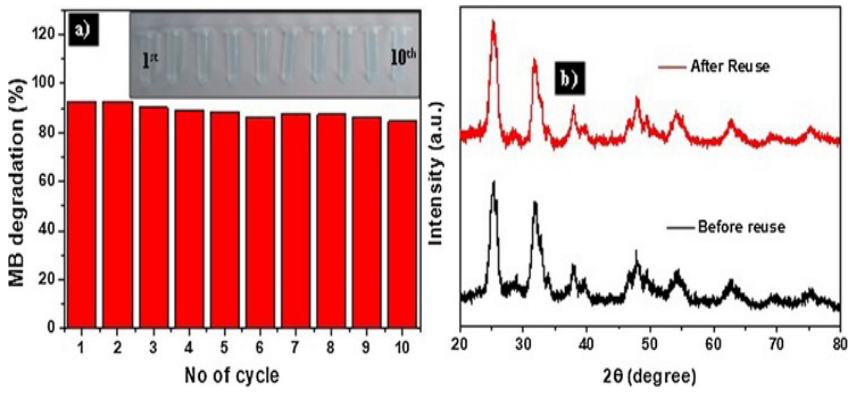

Figure 6 (a): Degradation efficiency of HAp-T nanoparticles after successive 10 cycles for degrading MB dye under UV light irradiation (inset shows the digital micrograph of MB solution after reaction for 10 times reuse); (b) XRD patterns of HAp-T nanoparticles before and after reusability test [145].

Photocatalysis is also used for degradation of antibiotics in wastewater. Xua, *et. al.* [146] fabricated a series of porous hollow HAp microspheres decorated with small amounts of ultrathin graphitic carbon nitride (g-C_3N_4) by a facile hydrothermal procedure. The photocatalytic efficiencies of the various g-C_3N_4/HAp composites were evaluated by degradation of tetracycline (TC). The results showed that g-C_3N_4/HAp composites can act as effective photocatalysts for TC degradation. Importantly, g-C_3N_4 (1.5 wt.%)/HAp composite displayed an excellent photocatalytic activity and good stability, which was faster than those over porous hollow HAp microspheres and ultrathin g-C_3N_4 solely. The presence of ultrathin g-C_3N_4 and porous hollow HAp microspheres in the g-C_3N_4/HAp composites promote the separation efficiency of the photogenerated electron-hole pairs, and thus resulting in high photocatalytic efficiency toward

TC degradation. Ekka, *et. al.* [147] prepared HAp decorated with zirconia nanoparticle (HAp-ZrO_2) by sonochemical method. It was found that the HAp-ZrO_2 nanocomposite exhibited effective photocatalytic activity towards the degradation of phenolic compounds (more than 95%). The improvement of photocatalytic activity for degradation of phenolic compounds may be because of the increase of specific surface area that provides the ordered adsorption and transport of charge carriers.

Sulaemana, *et. al.* [148] produced the high crystallinity of single phase Ag_3PO_4 based on HAp. Photocatalytic activities of the product were evaluated using Rhodamine B (RhB) decomposition under blue light irradiation. Ag_3PO_4/HAp decreases the particle size and generates the high absorption in the visible region. The photocatalytic activity of Ag_3PO_4/HAp increases up to 3.5 times higher compared to pure Ag_3PO_4. The mechanism of primary active species in the Ag_3PO_4 system works in the following order: $\bullet O_2^-$ > h+ > •OH and it was changed into the following order: h+ > $\bullet O_2^-$ > •OH in Ag_3PO_4/HAp.

Table 5 summarizes some applications of HAp-based composites for photocatalytic degradation of hazardous substances.

Table 5: Photo-catalytic degradation of hazardous materials by HAp composites

Materials	Synthesis methods	Degraded hazardous materials	Optimal catalytic conditions	Catalytic performance	Reference
V:HAp	Hydrothermal synthesis method	acetaldehyde	5% V:HAp	Quantum efficiency (number of reacted electron/number of absorbed photon) was 0.4% for the 5%-V:HAp calcined at 400 °C	[141]
Amorphous Fe (III)-substituted HAp	Ion-exchange method	rhodamine B	1.00 g of HAp was dispersed in 100 mL of 0.05 M $Fe(NO_3)_3$ solution	H_2O_2 (0.5 mM) existed, 86% of RhB was degraded after the 240 min irradiation	[143]
HAp-T	Sol-gel route	methylene blue	/	The degradation efficiency after 10 cycles of reuse was ~84.5%	[145]
g-C_3N_4/HAp	Facile hydrothermal procedure	tetracycline	g-C_3N_4 (1.5 wt.%)/ HAp	TC can be totally degraded by g-C_3N_4/HAp photocatalysts within 15 min	[146]
HAp-ZrO_2	Sonochemical method	phenol	/	degradation of phenols (above 95%)	[147]
Ag_3PO_4/HAp	coprecipitation	rhodamine B	/	/	[148]

6.2 Section summary

In this section, we introduce the applications of HAp-based composites with photocatalytic effect for degrading the organic pollutants in waste water. Further studies can be made between preparation, properties and specific applications. The deep connection among chemical composition, microstructure, band structure and photocatalytic material system is still need to be studied to improve the photocatalytic performance of HAp composites in a greater extent. In addition, the photocatalytic application regions of HAp should be extended to promoting its commercial application.

7. Chapter summary

HAp, its modification and composites are still significant important in research fields. HAp has been extensively used as a biomaterial because it has similar chemical composition with the inorganic part of natural bone. However, due to its unique microstructures, HAp has attracted broad attentions and has been studied and applied in many other fields besides biomedical materials, such as the environmental monitoring and treatment. For example, HAp can be used as a gas sensing material for detecting the environmental gases, an electrochemical sensor for detecting the heavy metals or inorganic substances in aqueous solution, an adsorbent for removing heavy metals in waste water and soil remediation, as well as a photocatalyst for degrading organic pollutants in waste water. However, the application fields of HAp are not limited to the content described in this chapter. Thus, HAp is a very important and promising material. However, in the future, more efforts are still needed to be made to promote the transformation of scientific research achievement into the commercial products by the researchers from both of the academic and industrial fields. Thus, more works are still needed to be done in order to meet the requirements of commercial application including fully understanding the mechanisms, improving the properties, performance, efficiency and stability of the product, and reducing the cost of the product, and so on.

8. Acknowledgement

This work was financially supported by National Natural Science Foundation of China (51504295), Hunan Provincial Natural Science Foundation of China (2019JJ50797), the project of Innovation and Entrepreneur Team Introduced by Guangdong Province (201301G0105337290), and the Special Funds for Future Industrial Development of Shenzhen (No. HKHTZD20140702020004), Yuanmeng Precision Technology (Shenzhen) Institute, Shenzhen, China.

9. References

1. Dorozhkin SV, Epple M. Biological and medical significance of calcium phosphates. Angewandte Chemie International Ed in English. 2002;41(17):3130-46.

2. Fratzl P, Gupta HS, Paschalis EP, Roschger P. Structure and mechanical quality of the collagen–mineral nano-composite in bone. Journal of Materials Chemistry. 2004;14(14):2115-23.

3. Paul W, Sharma CP. Development of porous spherical hydroxyapatite granules: application towards protein delivery. Journal of Materials Science: Materials in Medicine. 1999;10(7):383-8.

4. Uskokovic V, Uskokovic DP. Nanosized hydroxyapatite and other calcium phosphates: chemistry of formation and application as drug and gene delivery agents. Journal of Biomedical Materials Research Part B: Applied Biomaterials. 2011;96(1):152-91.

5. Watanabe Y, Ikoma T, Suetsugu Y, Yamada H, Tamura K, Komatsu Y, et al. The densification of zeolite/apatite composites using a pulse electric current sintering method: A long-term assurance material for the disposal of radioactive waste. Journal of the European Ceramic Society. 2006;26(4-5):481-6.

6. Ternane R, Trabelsi-Ayedi M, Kbir-Ariguib N, Piriou B. Luminescent properties of Eu3+ in calcium hydroxyapatite. Journal of Luminescence. 1999;81(3):165-70.

7. Huixia L, Yong L, Yanni T, Lanlan L, Qing Z, Kun L, et al. Room temperature gas sensing properties of tubular hydroxyapatite. New Journal of Chemistry. 2015;39(5):3865-74.

8. Feng Y, Gong J-L, Zeng G-M, Niu Q-Y, Zhang H-Y, Niu C-G, et al. Adsorption of Cd (II) and Zn (II) from aqueous solutions using magnetic hydroxyapatite nanoparticles as adsorbents. Chemical Engineering Journal. 2010;162(2):487-94.

9. Boukha Z, González-Prior J, Rivas Bd, González-Velasco JR, López-Fonseca R, Gutiérrez-Ortiz JI. Synthesis, characterisation and behaviour of Co/hydroxyapatite catalysts in the oxidation of 1,2-dichloroethane. Applied Catalysis B: Environmental. 2016;190:125-36.

10. Fihri A, Len C, Varma RS, Solhy A. Hydroxyapatite: A review of syntheses, structure and applications in heterogeneous catalysis. Coordination Chemistry Reviews. 2017;347:48-76.

11. LeGeros RZ, LeGeros JP. Dense hydroxyapatite. An Introduction to Bioceramics1993. p. 139-80.

12. Malmberg P, Nygren H. Methods for the analysis of the composition of bone tissue, with a focus on imaging mass spectrometry (TOF-SIMS). Proteomics. 2008;8(18):3755-62.

13. Kay MI, Young RA, Posner AS. Crystal structure of hydroxyapatite. Nature. 1964;204:1050-2.

14. Carrodeguas RG, De Aza S. alpha-Tricalcium phosphate: Synthesis, properties and biomedical applications. Acta Biomaterialia. 2011;7(10):3536-46.

15. Okada M, Matsumoto T. Synthesis and modification of apatite nanoparticles for use in dental and medical applications. Japanese Dental Science Review. 2015;51(4):85-95.

16. Sadat-Shojai M, Khorasani MT, Dinpanah-Khoshdargi E, Jamshidi A. Synthesis methods for nanosized hydroxyapatite with diverse structures. Acta Biomaterialia. 2013;9(8):7591-621.

17. Fowler BO. Infrared studies of apatites. II. Preparation of normal and isotopically substituted calcium, strontium, and barium hydroxyapatites and spectra-structure-composition correlations. Inorganic Chemistry. 1974;13(1):207-14.

18. Güler H, Gündoğmaz G, Kurtuluş F, Çelik G, Gacanoğlu ŞS. Solid state synthesis of calcium borohydroxyapatite. Solid State Sciences. 2011;13(11):1916-20.

19. Rao RR, Roopa HN, Kannan TS. Solid state synthesis and thermal stability of HAP and HAP – β-TCP composite ceramic powders. Journal of Materials Science: Materials in Medicine. 1997;8(8):511-8.

20. Safavi A, Sorouri M. Multiwalled carbon nanotube wrapped hydroxyapatite, convenient synthesis via microwave assisted solid state metathesis. Materials Letters. 2013;91:287-90.

21. Teshima K, Lee S, Sakurai M, Kameno Y, Yubuta K, Suzuki T, et al. Well-formed one-dimensional hydroxyapatite crystals grown by an environmentally friendly flux method. Crystal Growth & Design. 2009;9(6):2937-40.

22. Zhang HG, Zhu Q. Preparation of fluoride-substituted hydroxyapatite by a molten salt synthesis route. Journal of Materials Science: Materials in Medicine. 2006;17(8):691-5.

23. Bakan F, Laçin O, Sarac H. A novel low temperature sol–gel synthesis process for thermally stable nano crystalline hydroxyapatite. Powder Technology. 2013;233:295-302.

24. Nagai M, Nishino T, Saeki T. A new type of CO2 gas sensor comprising porous hydroxyapatite ceramics. Sensors and Actuators. 1988;15(2):145-51.

25. Mahabole MP, Aiyer RC, Ramakrishna CV, Sreedhar B, Khairnar RS. Synthesis, characterization and gas sensing property of hydroxyapatite ceramic. Bulletin of Materials Science. 2005;28(6):535-45.

26. Khairnar RS, Mene RU, Munde SG, Mahabole MP, Iskandar F, Abdullah M. Nano-hydroxyapatite thick film gas sensors. The 4th Nanoscience and Nanotechnolgy symposium (NNS-2011); Bali, Indonesia: American Institute of Physics; 2011. p. 189-92.

27. Mene RU, Mahabole MP, Sharma R, Khairnar RS. Enhancement in CO gas sensing properties of hydroxyapatite thick films: Effect of swift heavy ion irradiation. Vacuum. 2011;86(1):66-71.

28. Luo L, Liu Y, Tan Y, Li H, Zhang Q, Li K. Room temperature gas sensor based on tube-like hydroxyapatite modified with gold nanoparticles. Journal of Central South University. 2016;23(1):18-26.

29. Tan Y, Li H, Liu Y, Xie J, He J, Pan J. Acidithiobacillus ferrooxidans improved H2S gas sensing properties of tubular hydroxyapatite at room temperature. RSC Advances. 2016;6(80):76874-8.

30. Nakamura S, Takeda H, Yamashita K. Proton transport polarization and depolarization of hydroxyapatite ceramics. Journal of Applied Physics. 2001;89(10):5386-92.

31. Zhang HG, Zhu Q. Preparation of fluoride-substituted hydroxyapatite by a molten salt synthesis route. J Mater Sci Mater Med. 2006;17(8):691-5.

32. He B, Zhen X, Wen H, Wang S. Antagonistic action of organic selenium on lead poisoning. Journal of Hygiene Research. 1998;27(4):229.

33. Miaomiao Q. Research progress of environmental cadmium exposure to human health injury. Health research. 2007;36(2):255-7.

34. Qin Junfa LZ. Human health effects of cadmium. Guangdong science of trace elements. 2004;11(6):1-10.

35. Huang Qiuchan WY, Li Xiaofeng. Research progress on the harmful effects of cadmium on human health and its mechanism. Anhui agricultural science. 2007;35(9):2528-31.

36. Zhang Y, Liu Y, Ji X, Banks CE, Zhang W. Conversion of egg-shell to hydroxyapatite for highly sensitive detection of endocrine disruptor bisphenol A. Journal of Materials Chemistry. 2011;21(38):14428-31.

37. Bai Aimei LY, Fan Zhongxue. Arsenic is harmful to human health. Research on trace elements and health. 2007;24(1):61-2.

38. Huang Qiuchan WY, Wu YIngzhen. Study on the harmful effects of arsenic pollution on human health. Research on

trace elements and health. 2009;26(4):65-7.

39. Wang Xiuhong BJ. Trace element arsenic and human health. Foreign medicine (medical geography). 2005;26(3):101-5.

40. Jiaojiao S. Heavy metal contamination in water - chromium. 2012(11).

41. Plum LM, Rink L, Haase H. The essential toxin: impact of zinc on human health. Int J Environ Res Public Health. 2010;7(4):1342-65.

42. Morris DR, Levenson CW. Ion channels and zinc: mechanisms of neurotoxicity and neurodegeneration. Journal of Toxicology. 2012;2012(5):785647.

43. Aizenman E, Stout AK, Hartnett KA, Dineley KE, Mclaughlin BA, Reynolds IJ. Induction of neuronal apoptosis by thiol oxidation. Journal of Neurochemistry. 2010;75(5):1878-88.

44. Nriagu J. Zinc toxicity in humans. Encyclopedia of Environmental Health. 2011;20(4):801-7.

45. María Eugenia L, Ana María L, Mario F, Julia S, Rigoberto M, Paula A, et al. Possible mechanisms underlying copper-induced damage in biological membranes leading to cellular toxicity. Chemico-Biological Interactions. 2005;151(2):71-82.

46. Ivask A, Juganson K, Bondarenko O, Mortimer M, Aruoja V, Kasemets K, et al. Mechanisms of toxic action of Ag, ZnO and CuO nanoparticles to selected ecotoxicological test organisms and mammalian cells in vitro: A comparative review. Nanotoxicology. 2014;8(sup1):57-71.

47. Corami A, Mignardi S, Ferrini VJJCIS. Cadmium removal from single- and multi-metal (Cd+Pb+Zn+Cu) solutions by sorption on hydroxyapatite. Journal of Colloid and Interface Science. 2008;317(2):402-8.

48. Bontidean I, Berggren C, Johansson G, Csöregi E, Mattiasson B, Lloyd JR, et al. Detection of heavy metal ions at femtomolar levels using protein-based biosensors. Analytical Chemistry. 1998;70(19):4162-9.

49. Chao G, Huang XJ. Voltammetric determination of mercury(II). Trends in Analytical Chemistry. 2013;51(51):1-12.

50. Li Y, Liu XR, Ning XH, Huang CC, Zheng JB, Zhang JC. An ionic liquid supported CeO nanoparticles–carbon nanotubes composite-enhanced electrochemical DNA-based sensor for the detection of Pb. Journal of Pharmaceutical Analysis. 2011;1(4):258-63.

51. Bansod B, Kumar T, Thakur R, Rana S, Singh I. A review on various electrochemical techniques for heavy metal ions detection with different sensing platforms. Biosens Bioelectron. 2017;94:443-55.

52. Gumpu MB, Sethuraman S, Krishnan UM, Rayappan JBB. A review on detection of heavy metal ions in water – An electrochemical approach. Sensors and Actuators B: Chemical. 2015;213:515-33.

53. Lu Y, Liang X, Niyungeko C, Zhou J, Xu J, Tian G. A review of the identification and detection of heavy metal ions in the environment by voltammetry. Talanta. 2018;178:324-38.

54. Dias JM, Alvimferraz MC, Almeida MF, Riverautrilla J, Sánchezpolo. Waste materials for activated carbon preparation and its use in aqueous-phase treatment: a review. Journal of Environmental Management. 2007;85(4):833-46.

55. Demirbas. Heavy metal adsorption onto agro-based waste materials: a review. Journal of Hazardous Materials. 2008;157(2):220-9.

56. Dias JM, Alvimferraz MC, Almeida MF, Riverautrilla J, Sánchezpolo MJJoEM. Waste materials for activated carbon preparation and its use in aqueous-phase treatment: a review. 2007;85(4):833-46.

57. Demirbas AJJoHM. Heavy metal adsorption onto agro-based waste materials: a review. 2008;157(2):220-9.

58. Radin SR, Ducheyne. The effect of calcium phosphate ceramic composition and structure on in vitro behavior. II. Precipitation. Journal of Biomedical Materials Research Part A. 1993;27(1):35-45.

59. Koutsopoulos S. Synthesis and characterization of hydroxyapatite crystals: a review study on the analytical methods. Journal of Biomedical Materials Research Part A. 2010;62(4):600-12.

60. Tsuchida T, Kubo J, Yoshioka T, Sakuma S, Takeguchi T, Ueda W. Reaction of ethanol over hydroxyapatite affected by Ca/P ratio of catalyst. Journal of Catalysis. 2008;259(2):183-9.

61. Elliott JC. Structure and chemistry of the apatites and other calcium orthophosphates. Amsterdam: Elsevier; 1994.

62. Koutsopoulos S. Synthesis and characterization of hydroxyapatite crystals: a review study on the analytical methods. Journal of Biomedical Materials Research Part A. 2010;62(4):-.

63. Tsuchida T, Kubo J, Yoshioka T, Sakuma S, Takeguchi T, Ueda WJJoC. Reaction of ethanol over hydroxyapatite affected by Ca/P ratio of catalyst. 2008;259(2):183-9.

64. Mousa SM, Ammar NS, Ibrahim HA. Removal of lead ions using hydroxyapatite nano-material prepared from phosphogypsum waste. Journal of Saudi Chemical Society. 2016;20(3):357-65.

65. Reichert J, Binner JGP. An evaluation of hydroxyapatite-based filters for removal of heavy metal ions from aqueous solutions. Journal of Materials Science. 1996;31(5):1231-41.

66. Ma QY, Traina SJ, Logan TJ, Ryan JA. Effects of Aqueous Al, Cd, Cu, Fe(II), Ni, and Zn on Pb Immobilization by Hydroxyapatite. Environmental Science&Technology. 1994;28(7):1219-28.

67. Batton J, Kadaksham AJ, Nzihou A, Singh P, Aubry N. Trapping heavy metals by using calcium hydroxyapatite and dielectrophoresis. Journal of Hazardous Materials. 2007;139(3):461-6.

68. Campisi S, Castellano C, Gervasini A. Tailoring structural and morphological properties of hydroxyapatite materials to enhance the capture efficiency towards copper(II) and lead(II) ions. New Journal of Chemistry. 2018;42(6):11-7.

69. Zhang Y, Liu Y, Ji X, Banks CE, Zhang W. Conversion of natural egg-shell to 3D flower-like hydroxyapatite agglomerates for highly sensitive detection of As3+ ions. Materials Letters. 2012;78:120-3.

70. Zhang Y, Liu Y, Ji X, Banks CE, Zhang W. Flower-like hydroxyapatite modified carbon paste electrodes applicable for highly sensitive detection of heavy metal ions. Journal of Materials Chemistry. 2011;21(21):7552-4.

71. Zhang Y, Liu Y, Ji X, Banks CE, Zhang W. Sea cucumber-like hydroxyapatite: cation exchange membrane-assisted synthesis and its application in ultra-sensitive heavy metal detection. Chemistry Communication (Camb). 2011;47(14):4126-8.

72. Prongmanee W, Alam I, Asanithi P. Hydroxyapatite/Graphene oxide composite for electrochemical detection of L-Tryptophan. Journal of the Taiwan Institute of Chemical Engineers. 2019:415-23.

73. Pang P, Liu Y, Zhang Y, Gao Y, Hu Q. Electrochemical determination of luteolin in peanut hulls using graphene and hydroxyapatite nanocomposite modified electrode. Sensors and Actuators B:Chemical. 2014;194(4):397-403.

74. Ajab H, Ali Khan AA, Nazir MS, Yaqub A, Abdullah MA. Cellulose-hydroxyapatite carbon electrode composite for trace plumbum ions detection in aqueous and palm oil mill effluent: Interference, optimization and validation studies. Environmental Research. 2019;176:108563.

75. Ajab H, Dennis JO, Abdullah MA. Synthesis and characterization of cellulose and hydroxyapatite-carbon electrode composite for trace plumbum ions detection and its validation in blood serum. International Journal of Biological Macromolecules. 2018;113:376-85.

76. Frantseska-Maria P, Apostolos G, Dimitrios K, Kalliopi A, Rainer S, Jing-Yuan W, et al. Adsorption of Cu(II) ions from aqueous solutions on biochars prepared from agricultural by-products. Journal of Environmental Management.

2012;96(1):35-42.

77. Diógenes T, Mendonça K, Guerra RO. Chemical nature of carbonaceous materials from biomass by hydrothermal carbonization and low temperature conversion. Journal of Biobased Materials&Bioenergy. 2013;7(3):367-75.

78. Wang H, You NC, Wei Y. A novel magnetic calcium silicate/graphene oxide composite material for selective adsorption of acridine orange from aqueous solutions. RSC Advances. 2016;6(41):34770-81.

79. Papageorgiou SK, Katsaros FK, Kouvelos EP, Kanellopoulos NK. Prediction of binary adsorption isotherms of Cu(2+), Cd(2+) and Pb(2+) on calcium alginate beads from single adsorption data. Journal of Hazardous Materials. 2009;162(2):1347-54.

80. Mobasherpour I, Salahi E, Pazouki M. Removal of nickel (II) from aqueous solutions by using nano-crystalline calcium hydroxyapatite. Journal of Saudi Chemical Society. 2011;15(2):105-12.

81. Zhou H, Lee J. Nanoscale hydroxyapatite particles for bone tissue engineering. Acta Biomaterialia. 2011;7(7):2769-81.

82. Li Z, Zhou M-m, Lin W. The research of nanoparticle and microparticle hydroxyapatite amendment in multiple heavy metals contaminated soil remediation. Journal of Nanomaterials. 2014.

83. Li J, Wang X, Zhao G, Chen C, Wang X. Metal-organic framework-based materials: Superior adsorbents for the capture of toxic and radioactive metal ions. Chemical Society Reviews. 2018;47(Part 1).

84. Gu P, Zhang S, Li X, Wang X, Wen T, Jehan R, et al. Recent advances in layered double hydroxide-based nanomaterials for the removal of radionuclides from aqueous solution. Environmental Pollution. 2018;240:493-505.

85. Zhao G, Huang X, Tang Z, Huang Q, Wang XK. Polymer-based nanocomposites for heavy metal ions removal from aqueous solution: A review. Polymer Chemistry. 2018;9(26):3562-82.

86. Takeuchi Y, Sato M, Suzuki H. New concept of machining by means of six-axis control. CIRP Annals - Manufacturing Technology. 1994;43(1):341-4.

87. Cipitria A, Reichert JC, Epari DR, Saifzadeh S, Berner A, Schell H, et al. Polycaprolactone scaffold and reduced rhBMP-7 dose for the regeneration of critical-sized defects in sheep tibiae. Biomaterials. 2013;34(38):9960-8.

88. Skwarek E. Adsorption of Zn on Synthetic Hydroxyapatite from Aqueous Solution. Separation Science and Technology. 2014;49(11):1654-62.

89. Janusz W, Skwarek E. Study of sorption processes of strontium on the synthetic hydroxyapatite. Adsorption-Journal of the International Adsorption Society. 2016;22(4-6):697-706.

90. Skwarek E, Goncharuk O, Sternik D, Janusz W, Gdula K, Gun'ko VM. Synthesis, structural, and adsorption properties and thermal stability of nanohydroxyapatite/polysaccharide composites. Nanoscale Research Letters. 2017;12.

91. Skwarek E, Janusz W. Adsorption of Cd(II) ions at the hydroxyapatite/electrolyte solution interface. Separation Science and Technology. 2016;51(1):11-21.

92. Janusz W, Skwarek E. Effect of Co(II) ions adsorption in the hydroxyapatite/aqueous NaClO4 solution system on particles electrokinetics. Physicochemical Problems of Mineral Processing. 2018;54(1):31-9.

93. Skwarek E, Janusz W. Adsorption of Ba2+ ions at the hydroxyapatite/NaCl solution interface. Adsorption-Journal of the International Adsorption Society. 2019;25(3):279-88.

94. Skwarek E, Gladysz-Plaska A, Choromanska JB, Broda E. Adsorption of uranium ions on nano-hydroxyapatite and modified by Ca and Ag ions. Adsorption-Journal of the International Adsorption Society. 2019;25(3):639-47.

95. Guo H, Jiang C, Xu Z, Luo P, Fu Z, Zhang J. Synthesis of bitter gourd-shaped nanoscaled hydroxyapatite and its

adsorption property for heavy metal ions. Materials Letters. 2019;241:176-9.

96. Xing L, Yang L, Zhang C, Tao W, Li Z, Wang X, et al. Porous Fe2O3 microcubes derived from metal organic frameworks for efficient elimination of organic pollutants and heavy metal ions. Chemical Engineering Journal. 2017;336:241-52.

97. Wang XK, Gu P, Xing J, Tao W, Rui Z, Jian W, et al. Experimental and theoretical calculation investigation on efficient Pb(II) adsorption to etched Ti3AlC2 nanofibers and nanosheets. Environmental Science Nano. 2018;5(4):946-55.

98. Zhu H, Tan X, Tan L, Zhang H, Liu H, Ming F, et al. Magnetic porous polymers prepared via high internal phase emulsions for efficient removal of Pb2+ and Cd2+. ACS Sustainable Chemistry&Engineering. 2018;6(4):5206-13.

99. Xing L, Xing J, Zhang C, Bing H, Wang X. Adsorption of lead on sulfur-doped graphitic carbon nitride nanosheets: experimental and theoretical calculation study. ACS Sustainable Chemistry&Engineering. 2018;6(8).

100. Wardle DA, Marie-Charlotte N, Olle Z. Fire-derived charcoal causes loss of forest humus. Science(NEW YORK). 2008;320(5876):629-.

101. Zimmerman AR, Gao B, Ahn MY. Positive and negative carbon mineralization priming effects among a variety of biochar-amended soils. Soil Biology and Biochemistry. 2011;43(6):1169-79.

102. Mohan D, Sarswat A, Ok YS, Jr PC. Organic and inorganic contaminants removal from water with biochar, a renewable, low cost and sustainable adsorbent--a critical review. Bioresource Technology. 2014;160(5):191-202.

103. Zhou Y, Gao B, Zimmerman AR, Fang J, Sun Y, Cao X. Sorption of heavy metals on chitosan-modified biochars and its biological effects. Chemical Engineering Journal. 2013;231(9):512-8.

104. Wang Y-Y, Liu Y-X, Lu H-H, Yang R-Q, Yang S-M. Competitive adsorption of Pb(II), Cu(II), and Zn(II) ions onto hydroxyapatite-biochar nanocomposite in aqueous solutions. Journal of Solid State Chemistry. 2018;261:53-61.

105. Guo J, Han Y, Mao Y, Wickramaratne MN. Influence of alginate fixation on the adsorption capacity of hydroxyapatite nanocrystals to Cu2+ ions. Colloids and Surfaces A: Physicochemical and Engineering Aspects. 2017;529:801-7.

106. GOOGERDCHIAN, Fahimeh, MOHEB, Ahmad, EMADI, Rahmatollah. Lead sorption properties of nanohydroxyapatite-alginate composite adsorbents. Chemical Engineering Journal. 2012;200-202:471---9.

107. Gabr RM, Gad-Elrab SMF, Abskharon RNN, Hassan SHA, Shoreit AAM. Biosorption of hexavalent chromium using biofilm of E. coli supported on granulated activated carbon. World Journal of Microbiology and Biotechnology. 2009;25(10):1695-703.

108. Piccirillo C, Pereira SI, Marques AP, Pullar RC, Tobaldi DM, Pintado ME, et al. Bacteria immobilisation on hydroxyapatite surface for heavy metals removal. Journal of Environmental Management. 2013;121:87-95.

109. Piccirillo C, Silva MF, Pullar RC, Cruz IBD, Jorge R, Pintado MME, et al. Extraction and characterisation of apatite- and tricalcium phosphate-based materials from cod fish bones. Materials Science Engineering:C-Materials for biological applications. 2013;33(1):103-10.

110. Boisson J, Ruttens A, Mench M, Vangronsveld J. Evaluation of hydroxyapatite as a metal immobilizing soil additive for the remediation of polluted soils. Part 1. Influence of hydroxyapatite on metal exchangeability in soil, plant growth and plant metal accumulation. Environmental Pollution. 1999;104(2):225-33.

111. . !!! INVALID CITATION !!! (107-109).

112. Xia W-Y, Du Y-J, Li F-S, Guo G-L, Yan X-L, Li C-P, et al. Field evaluation of a new hydroxyapatite based binder for ex-situ solidification/stabilization of a heavy metal contaminated site soil around a Pb-Zn smelter. Construction and Building Materials. 2019;210:278-88.

113. Wang Y, Li R, Liu W, Cheng L, Jiang Q, Zhang Y. Exploratory of immobilization remediation of hydroxyapatite

(HAP) on lead-contaminated soils. Environmental science and pollution research international. 2019:1-11.

114. Zhu F, He S, Shang Z. Effect of vegetables and nano-particle hydroxyapatite on the remediation of cadmium and phosphatase activity in rhizosphere soil through immobilization. International Journal of Phytoremediation. 2019;21(6):610-6.

115. Wang L, Li Y-h, Ji Y-f, Yang L-s, Li H-r, Zhang X-w, et al. Remediation Pb, Cd Contaminated Soil in Lead-zinc Mining Areas by Hydroxyapatite and Potassium Chloride Composites. Huanjing Kexue. 2011;32(7):2114-8.

116. He M, Shi H, Zhao X, Yu Y, Qu B. Immobilization of Pb and Cd in Contaminated Soil Using Nano-Crystallite Hydroxyapatite. Procedia Environmental Sciences. 2013;18:657-65.

117. Yang Z, Fang Z, Zheng L, Cheng W, Tsang PE, Fang J, et al. Remediation of lead contaminated soil by biochar-supported nano-hydroxyapatite. Ecotoxicology and Environmental Safety. 2016;132:224-30.

118. Liu H, Zhang Y, Chen N, Liu G, Cui H, Liang J, et al. Effect of surface characteristics of hydroxyapatite on the remediation passivation effect of heavy metal contaminated soil. Huanjing Huaxue-Environmental Chemistry. 2018;37(9):1961-70.

119. Xue J, Wang. J. Radiolysis of pentachlorophenol (PCP) in aqueous solution by gamma radiation. Journal of Environmental Sciences. 2008;20(10):1153-7.

120. Sax NI. Dangerous properties of industrial materials. American Journal of Public Health:the Nations Health. 1979;49(1):140.

121. Martín J, Camacho-Muñoz D, Santos JL, Aparicio I, Alonso E. Occurrence of pharmaceutical compounds in wastewater and sludge from wastewater treatment plants: Removal and ecotoxicological impact of wastewater discharges and sludge disposal. Journal of Hazardous Materials. 2012;239-240(none):40-7.

122. Huber MM, Silvio C, Gun-Young P, Urs VG. Oxidation of pharmaceuticals during ozonation and advanced oxidation processes. Environmental Science&Technology. 2003;37(5):1016-24.

123. Boczkaj G, Fernandes A. Wastewater treatment by means of advanced oxidation processes at basic pH conditions: A review. Chemical Engineering Journal. 2017;320:608-33.

124. Reddy PAK, Reddy PVL, Kwon E, Kim KH, Akter T, Kalagara S. Recent advances in photocatalytic treatment of pollutants in aqueous media. Chemical Engineering Journal. 2016;91:94-103.

125. Zhao J, Chen C, Ma W. Photocatalytic degradation of organic pollutants under visible light irradiation. Topics in Catalysis. 2005;35(3-4):269-78.

126. Gaya UI, Abdullah AH. Heterogeneous photocatalytic degradation of organic contaminants over titanium dioxide: A review of fundamentals, progress and problems. Journal of Photochemistry and Photobiology C:Photochemistry Reviews. 2008;9(1):1-12.

127. Lee KM, Lai CW, Ngai KS, Juan JC. Recent developments of zinc oxide based photocatalyst in water treatment technology: A review. Water Research. 2016;88:428-48.

128. Nzihou A, Sharrock P. Role of phosphate in the remediation and reuse of heavy metal polluted wastes and sites. Waste and Biomass Valorization. 2010;1(1):163-74.

129. Xinde C, Ma LQ, Rhue DR, Appel CS. Mechanisms of lead, copper, and zinc retention by phosphate rock. Environmental Pollution. 2004;131(3):435-44.

130. Agnieszka D, Manning DAC, Collins MJ, Timothy W, Stephen W, Eugenia VJ. An evaluation of the reactivity of synthetic and natural apatites in the presence of aqueous metals. Science of the Total Environment. 2009;407(8):2953-65.

131. Lin K, Pan J, Chen Y, Cheng R, Xu X. Study the adsorption of phenol from aqueous solution on hydroxyapatite nanopowders. Journal of Hazardous Materials. 2009;161(1):231-40.

132. Bouyarmane H, Hanbali IE, Karbane ME, Rami A, Saoiabi A, Saoiabi S, et al. Parameters influencing ciprofloxacin, ofloxacin, amoxicillin and sulfamethoxazole retention by natural and converted calcium phosphates. Journal of Hazardous Materials. 2015;291:38-44.

133. Karima A, Sylvie M, Guillaume L, Cécile R, Abdelaziz L, Ahmed S, et al. Ultrasound-assisted synthesis of mesoporous zirconia-hydroxyapatite nanocomposites and their dual surface affinity for Cr3+/Cr2O7(2-) ions. Langmuir :The ACS journal of surfaces and colloids. 2011;27(24):15176-84.

134. Yang H, Masse S, Rouelle M, Aubry E, Li Y, Roux C, et al. Magnetically recoverable iron oxide–hydroxyapatite nanocomposites for lead removal. International Journal of Environmental Science and Technology. 2015;12(4):1173-82.

135. Nakajima A, Takakuwa K, Kameshima Y, Hagiwara M, Sato S, Yamamoto Y, et al. Preparation and properties of titania–apatite hybrid films. Journal of Photochemistry and Photobiology A:Chemistry. 2006;177(1):94-9.

136. Sheng G, Qiao L, Mou Y. Preparation of TiO2/hydroxyapatite composite and its photocatalytic degradation of methyl orange. Journal of Environmental Engineering. 2011;137(7):611-6.

137. Kandori K, Yamaguchi Y, Wakamura M. Photodecomposition of surfactants using Ti(IV)-doped calcium hydroxyapatite particles. Colloid and Polymer Science. 2017;295(6):1079-87.

138. Piccirillo C, Castro PML. Calcium hydroxyapatite-based photocatalysts for environment remediation: Characteristics, performances and future perspectives. Journal of Environmental Management. 2017;193:79-91.

139. Yagub MT, Sen TK, Afroze S, Ang HM. Dye and its removal from aqueous solution by adsorption: A review. Advances in Colloid and Interface Science. 2014;209(7):172-84.

140. Lian L, Guo L, Guo C. Adsorption of Congo red from aqueous solutions onto Ca-bentonite. Journal of Hazardous Materials. 2009;161(1):126-31.

141. Nishikawa M, Tan LH, Nakabayashi Y, Hasegawa T, Shiroishi W, Kawahara S, et al. Visible light responsive vanadium-substituted hydroxyapatite photocatalysts. Journal of Photochemistry and Photobiology A: Chemistry. 2015;311:30-4.

142. Ying D, Jing L, Lei S, Xu J, Wang X, Guo Z, et al. Graphene oxide–iron complex: synthesis, characterization and visible-light-driven photocatalysis. Journal of Materials Chemistry A. 2013;1(3):644-50.

143. Liu X, Ma J, Yang J. Visible-light-driven amorphous Fe(III)-substituted hydroxyapatite photocatalyst: Characterization and photocatalytic activity. Materials Letters. 2014;137:256-9.

144. Lee WLW, Lu CS, Lin HP, Chen JY, Chen CC. Photocatalytic degradation of ethyl violet dye mediated by TiO2 under an anaerobic condition. Journal of the Taiwan Institute of Chemical Engineers. 2014;45(5):2469-79.

145. Singh N, Chakraborty R, Gupta RK. Mutton bone derived hydroxyapatite supported TiO2 nanoparticles for sustainable photocatalytic applications. Journal of Environmental Chemical Engineering. 2018;6(1):459-67.

146. Xu T, Zou R, Lei X, Qi X, Wu Q, Yao W, et al. New and stable g-C3N4/HAp composites as highly efficient photocatalysts for tetracycline fast degradation. Applied Catalysis B: Environmental. 2019;245:662-71.

147. Ekka B, Nayak SR, Achary LSK, Sarita, Kumar A, Mawatwal S, et al. Synthesis of hydroxyapatite-zirconia nanocomposite through sonochemical route: A potential catalyst for degradation of phenolic compounds. Journal of Environmental Chemical Engineering. 2018;6(5):6504-15.

148. Sulaeman U, Suhendar S, Diastuti H, Riapanitra A, Yin S. Design of Ag3PO4 for highly enhanced photocatalyst using hydroxyapatite as a source of phosphate ion. Solid State Sciences. 2018;86:1-5.